

Nonlinear cyclic response of laminated glass FRP tubes filled with concrete

Yutian Shao, Amir Mirmiran *

Department of Civil Engineering, Constructed Facilities Laboratory, North Carolina State University, Raleigh, NC 27695-7533, USA

Available online 10 December 2003

Abstract

Fiber reinforced polymer (FRP) materials are generally known for their linear elastic response to failure. The present study evaluated the implications of using FRP as primary and sole reinforcement for concrete structures in seismic regions through an experimental and analytical investigation on the cyclic response of two different types of laminated glass FRP tubes filled with concrete. The study showed that concrete-filled tubes can be designed with an appropriate laminate structure for a ductility level comparable to that of conventional reinforced concrete columns. The nonlinearity and ductility in these types of structures stem from the off-axis response of the FRP tube. A hysteretic model was developed for the tube, and was cast into a two-dimensional three-node combined fiber element for the concrete-filled FRP tube. Good agreement was shown between the analytical models and the experimental results.

© 2003 Elsevier Ltd. All rights reserved.

Keywords: Composite tube; Cyclic loading; Ductility; Fiber orientation; Nonlinearity

1. Introduction

In recent years, a growing attention has been focused on the use of fiber reinforced polymers (FRP) in civil infrastructure applications. The driving force for these applications has been strong on both the demand and the supply sides of the equation. On the one hand, the civil engineering community, faced with the ever increasing problems of premature deterioration of traditional construction materials, has sought high performance materials to enhance safety and to prolong service life of the infrastructure facilities. On the other hand, the composites industry has pursued the infrastructure market in the face of declining demand in the defense industry.

Despite its successful introduction into the construction market, widespread acceptance of FRP by the civil engineering community has been slow not only by simple reluctance to the change of common practice, but also by many legitimate concerns. The economics of replacing traditional construction materials with ad-

vanced composites has been the most important factor in this regard. In fact, the two areas with most viable applications for FRP have been the repair of concrete structures and hybrid construction with concrete [1]. In both cases, FRP is used not as wholesale replacement of traditional construction materials, but rather to fortify them.

The legitimate technical concerns stem from the differences between the aerospace applications with civil engineering applications in regards to weathering, aging, and durability. The design life of aerospace components, for example, is typically around 60,000 h or 6.85 years [2]. This, however, is only a fraction of that needed in civil infrastructure [3]. Another important issue in civil engineering applications is the safety implications of using FRP materials in seismic regions. In order to avoid catastrophic failure of an entire structure, it is desired to dissipate energy by post-elastic deformations. However, FRP materials are generally known for their linear elastic response to failure. Therefore, it is important to evaluate the behavior of hybrid FRP-concrete structures under inelastic cyclic loading.

This paper shows the effect of FRP laminate structure on the seismic behavior of concrete-filled FRP tubes. The objectives of the present study were as follows:

* Corresponding author. Tel.: +1-919-513-1735; fax: +1-919-513-1765.

E-mail address: amir_mirmiran@ncsu.edu (A. Mirmiran).

- evaluate the feasibility of using FRP as external reinforcement for concrete columns in seismic regions; and
- determine whether or not additional internal steel reinforcement is required to develop plastic hinges in the structure.

2. Previous research

Research on FRP-concrete structures has been limited to the monotonic behavior of the system. To date, only a few studies have focused their attention on seismic applications of FRP in new construction. Seible et al. [4] reported tests on two columns made of concrete-filled carbon FRP tubes, both with 3.7 m height and 0.6 m inside diameter for the tube, under simulated seismic actions. One of the specimens with internal steel reinforcement at the column-footing joint performed superior to the conventional reinforced concrete column. On the other hand, the specimen without any internal steel reinforcement failed prematurely due to a combined state of compressive and inter-laminar shear stresses with very little energy dissipation capacity. They concluded that FRP alone would not be feasible for use in seismic regions, and that internal steel would be necessary to develop plastic hinge in a column or pile.

A similar approach was taken by Zhuo et al. [5]. They reported shaking table tests on reinforced concrete columns that were confined by glass FRP tubes. Two bridge models were tested, one with short columns at an aspect ratio (height-to-diameter ratio) of 2.5, and another with moderately long columns at an aspect ratio of 4. Test results indicated that the tubes did not increase the column strength, but greatly enhanced its hysteretic response up to a displacement ductility ratio of 10. Yamakawa et al. [6] reported similar observations on the seismic performance of square reinforced concrete columns that were confined with aramid FRP tubes. The common thread in all these studies has been the role of FRP as the secondary reinforcement, rather than sole replacement for steel bars. The primary reason for this approach has been the fundamental assumption that the FRP is incapable of producing a nonlinear ductile response.

On the other hand, and independently from the civil engineering community, significant research has taken place since the 1970s in the aerospace applications to determine the source, and to assess the magnitude of, nonlinearity in the off-axis direction in FRP structures. Hahn and Tsai [7] used a complementary energy density function to derive nonlinear relations for the in-plane shear. Hahn [8] extended the nonlinear theory of unidirectional lamina to that of laminated composites. Hu [9] reported that unidirectional FRP may exhibit severe nonlinearity in its in-plane shear stress–strain relation.

Also, some deviation from linearity may be observed under in-plane transverse loading, but the degree of nonlinearity is not comparable to that of the in-plane shear.

More recently, Haj-Ali and Kilic [10] carried out several coupon tests to calibrate three-dimensional micro-mechanical models for E-glass/vinyl-ester pultruded FRP. Tension, compression, and shear tests were performed on off-axis coupons cut at different angles of 0°, 15°, 30°, 45°, 60°, and 90°. The overall linear elastic properties were identified along with the nonlinear stress–strain behavior under the in-plane multi-axial tension and compression loading. The material had a lower ultimate tensile stress and initial stiffness in tension compared to the corresponding values from compression tests, regardless of thickness and orientation. This was attributed to the existing voids and micro-cracks that are more pronounced in the matrix-mode tensile loading. The difference between the compressive and tensile properties increased for off-axis angles approaching 90°.

Taking advantage of the off-axis behavior of FRP, Yuan et al. [11] proposed concrete-filled glass FRP tube with $\pm 45^\circ$ fiber orientation. No internal steel reinforcement was used. They reported that the FRP tube enhanced the strength of concrete by 2 1/2 times. Coupons of the tube showed bilinear response in tension and compression, with similar moduli of elasticity. However, the ultimate tensile strength was lower than the ultimate compressive strength. Most recently, Shao [12] completed several beam-column tests on concrete-filled FRP tubes, and showed the effect of laminate structure on the behavior of hybrid FRP-concrete system. The experimental program is discussed in the following section.

3. Experimental program

3.1. Hybrid FRP-concrete column tests

Six concrete-filled glass FRP tubes were tested under constant axial loading and reverse lateral loading in four point flexure [12]. Each specimen was 2.4 m long with 0.3 m inside diameter for the tube. Three of the tubes (W series) were made using centrifuge (spin) casting with 12.7 mm thickness and majority of the fibers in the longitudinal direction. The wall thickness in these tubes consisted of a 7.6 mm structural laminate with symmetric lay-up of 40 plies in the form of $[0^\circ/0^\circ/+45^\circ/-45^\circ]_{10}$ from E-glass and epoxy resin, a 4.6 mm resin-rich inner layer, and a 0.5 mm gel coating on the exterior. The other three tubes (Y series) were filament wound with 5 mm thickness and $\pm 55^\circ$ fiber orientation, also with E-glass and epoxy resin. However, these tubes did not have a resin layer nor a gel coating. Table 1 summarizes test data for each of the two tube series. In

Table 1
Test data for concrete-filled FRP tubes [12]

	Specimen series	
	W series	Y series
Tube inside diameter (mm)	279	312
Tube thickness (mm)	12.7	5.08
Tube tensile strength ^a (MPa)	399	71
Tube compressive strength ^a (MPa)	384	230
Tube tensile modulus ^a (GPa)	15.6	12.5
Tube compressive modulus ^a (GPa)	23.3	8.7
Laminate structure	[[0°/0°/±45°] ₁₀]	[[±55°] ₈ (55°)]
Glass content ^b	51.2%	75.5%
Fabrication method	Centrifuge (spin) casting	Filament winding

^a Manufacturer data.

^b Burnout tests.

each series, one specimen was prepared with no internal reinforcement, while the other two incorporated approximately 1.7% and 2.5% steel reinforcement ratios, respectively.

Loading was applied using a closed servo hydraulic system in displacement control with reversed motion from ±6.4 up to ±127 mm. Fig. 1 shows the loading regime, test setup, specimen cross sections and views of the specimens with their concrete end blocks in the upward and downward motions. Fig. 2 shows typical load–deflection hysteretic response curves and failure modes for the W and Y series, both without any internal steel reinforcement. The two types of tubes represented two different failure modes; a brittle compression failure for the W series with thick tubes and majority of the fibers in the longitudinal direction, and a ductile tension failure for the Y series with thin tubes and off-axis fibers. The hysteretic response curves clearly indicate little energy dissipation characteristics for the W series, whereas a ductile behavior is quite apparent from the wide loops

in the response of the Y series. Furthermore, an elasto-plastic behavior can be clearly seen from the envelope curve of the Y series.

Although not shown in the figure, the internal steel reinforcement improved the response of both types of tubes, but the effects were more pronounced with the Y series [12]. Moreover, the study showed that any internal steel in excess of 1–2% of the concrete core area may lead to premature crushing failure of the tube. General comparison of the concrete-filled FRP tubes of the Y series with conventional reinforced concrete columns indicated that hybrid FRP-concrete columns could be designed with a comparable ductile behavior [12]. Significant ductility can stem from the fiber architecture and the inter-laminar shear in the FRP tube.

In order to predict the hysteretic response of concrete-filled FRP tubes, an accurate model for the cyclic loading of FRP tubes is necessary. In the following sections, tests and modeling of coupons of the FRP tube are presented.

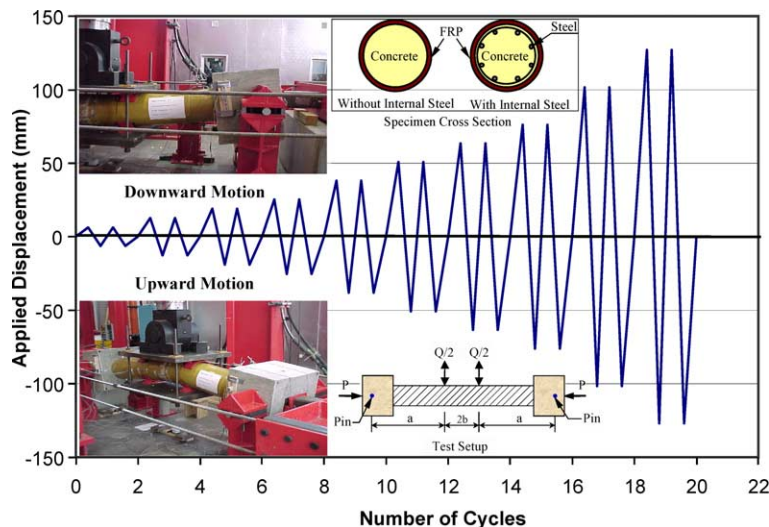


Fig. 1. Cyclic tests of hybrid FRP-concrete columns.

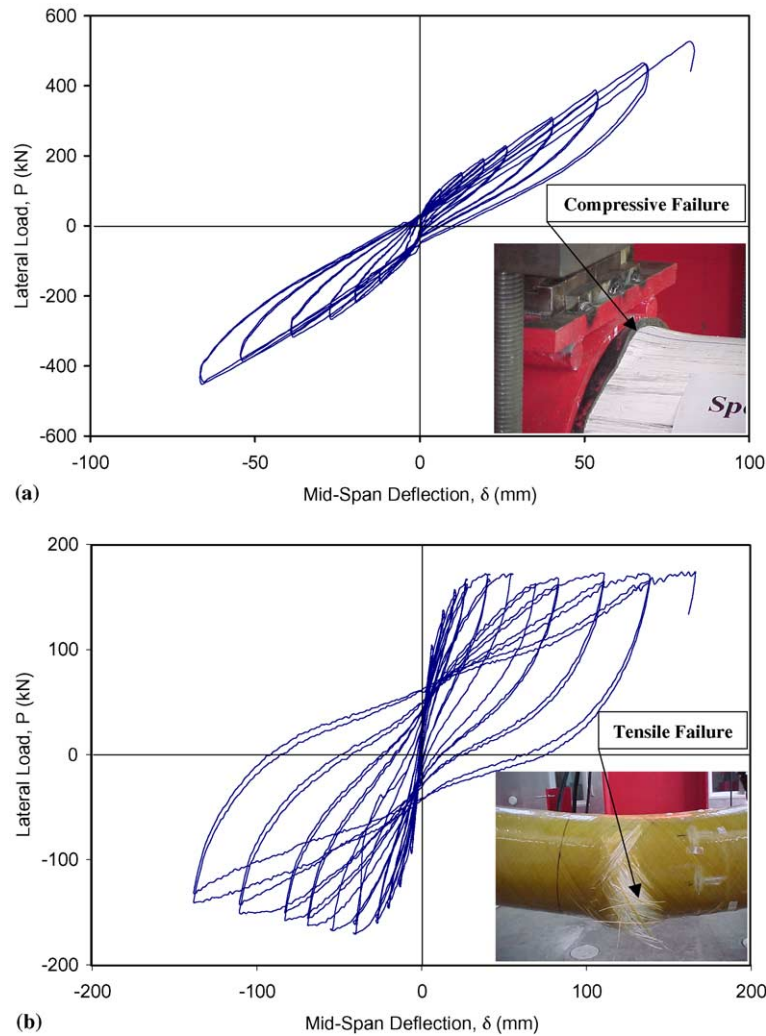


Fig. 2. Typical hysteretic response and failure modes of hybrid FRP-concrete columns: (a) W series and (b) Y series.

3.2. FRP coupon tests

Table 2 shows the test matrix and the dimensions of the FRP coupons. For each type of FRP tubes, four series of coupon testing were carried out: monotonic tension, monotonic compression, cyclic tension, and cyclic compression. Additional tests were carried out for the Y series with reverse cyclic loading in tension and compression. Uniaxial tension and compression tests followed the ASTM standards D3039-00 and D695-02a, respectively.

Fig. 3 shows typical failure modes of the coupons for the W and Y series in tension and compression. Failure mode for all tension coupons of the W series was identical, whether subjected to monotonic or cyclic loading (Fig. 3a). Prior to fiber rupture, cracking sound could be heard with increasing frequency. The sound was attributed to cracking of the resin-rich layer in the construct of the FRP tube. With the increased cracking of the resin, the load was transferred to the fibers. Failure was

always sudden, with a burst rupture of the fibers almost always at the mid-height of the coupons. Failure mode for the Y series in tension was distinctly different, in that there was no advance warning prior to failure (Fig. 3b). Moreover, failure was not accompanied by any noise nor any violent fiber rupture. Due primarily to the fiber orientation, the failure was predominantly controlled by the resin and the inter-laminar shear.

Failure mode for all compression coupons of the W series was identical, in that glass plies and the resin-rich inner layer separated at one end resembling a broom (Fig. 3c). Compression coupons of the Y series failed at their mid-heights, either in a horizontal direction or in the direction of the fibers (Fig. 3d). Careful observation revealed that the fracture lines on the two faces of each coupon were not at the same level. The axial compressive forces sheared off the resin for the most part. However, the direction of the resin failure depended on the imperfections of the laminate and the alignment of the fibers with respect to the loading plates.

Table 2
Test matrix for FRP coupons

	Specimen series			
	W series		Y series	
Type of loading	Tension	Compression	Tension	Compression
Number of monotonic tests	3	3	3	3
Number of cyclic tests	3	2	3	3
Number of reverse cyclic tests				2
Coupon width (mm)		38		38
Coupon length (mm)	305		305	
Coupon gage length (mm)	152		152	
Coupon thickness (mm)		12.7		5.1
Mode of failure	Fiber rupture	Lateral tear-off and local buckling	Shear	Shear

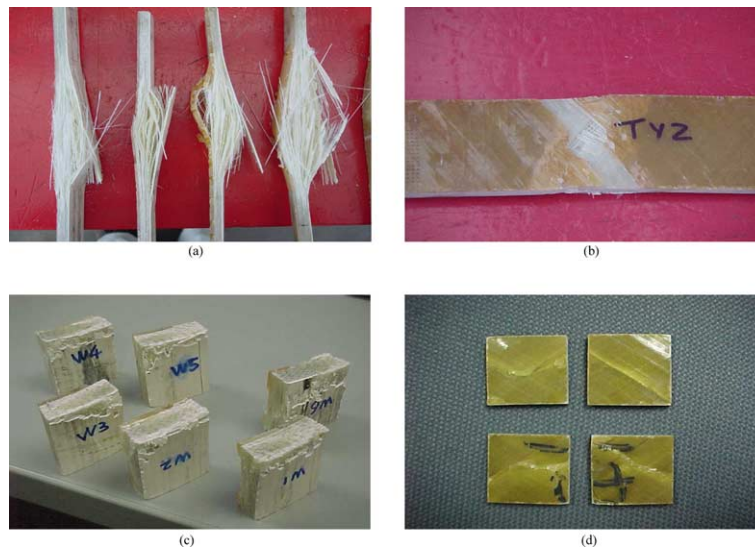


Fig. 3. Typical failure modes in coupon tests: (a) W series in tension, (b) Y series in tension, (c) W series in compression, and (d) Y series in compression.

Table 3 shows the average results for the FRP coupon tests. Fig. 4 shows typical stress–strain response of the W series in tension. The monotonic and cyclic responses are shown as thick and thin lines, respectively. The response is generally linear, particularly for the monotonic loading. The softening at about 20% of the capacity may be attributed to the fracture of the resin-rich inner layer. The unloading curves normally return

to the origin, with little or no plastic or residual strain. On the other hand, slight energy dissipation and stiffness degradation are observed during the unloading and reloading cycles.

Fig. 5 shows typical stress–strain response of the Y series in tension. Unlike the W series, significant non-linearity is apparent in both the monotonic and cyclic loading. The shape of the curve resembles a parabola.

Table 3
Average results of FRP coupon tests

	Specimen series			
	W series		Y series	
Type of loading	Tension	Compression	Tension	Compression
Ultimate strength (MPa)	517	414	44.8	159
Ultimate strain (mm/mm)	0.0230	0.0230	0.0045	0.0044
Tangent modulus of elasticity (GPa)	46.9	20.0	27.6	5.2
Secant modulus of elasticity (GPa)	22.4	20.0	10.3	3.9

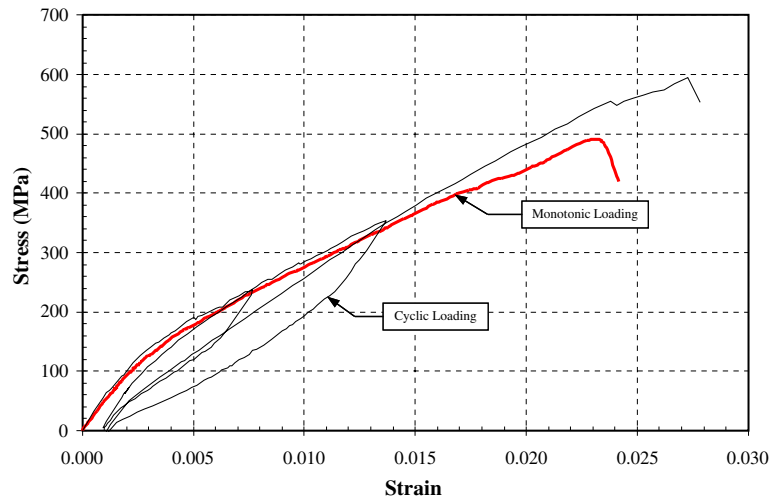


Fig. 4. Typical response of W series in tension.

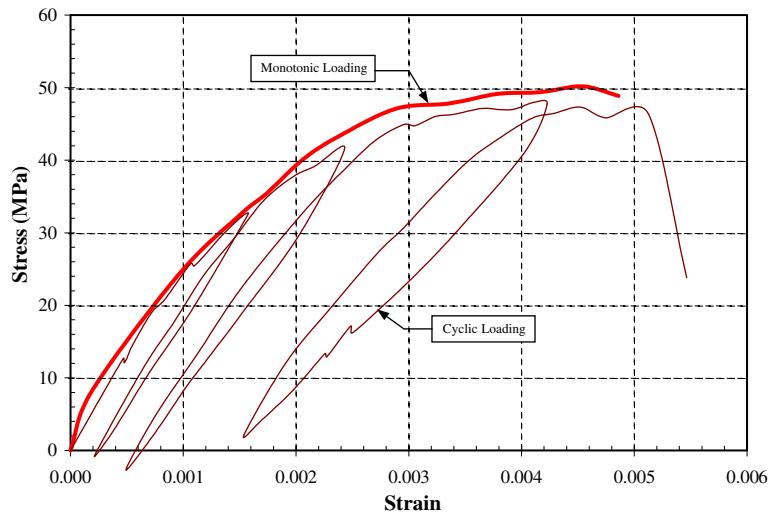


Fig. 5. Typical response of Y series in tension.

Energy dissipation during the unloading and reloading cycles is quite considerable. Plastic or residual strain after unloading and stiffness degradation upon reloading are both noticeable. On the other hand, strength and strain capacity of the Y series are much lower than those of the W series.

Fig. 6 shows typical stress–strain response of the W series in compression. The W series behaved almost linearly to failure, with essentially no plastic strain or energy dissipation. In fact, the linearity of the response of the W series is more apparent in compression than in tension. On the other hand, the strength and strain capacity of the W series in compression are slightly lower than those in tension. Moreover, the early softening of the response in tension does not appear in the compression loading.

Fig. 7 shows typical stress–strain response of the Y series in compression. The response is nonlinear with a parabolic shape. Plastic strains and the energy dissipation of the Y series in compression are much lower than those seen in tension. On the other hand, the strength and strain capacity of the Y series in compression are three and 10 times those of the same tubes in tension, respectively.

Fig. 8 depicts the typical response of the Y series under reverse cyclic loading in tension and compression. Due to limitations of the testing equipment, it was not feasible to provide adequate supports for lateral stability of the long coupon specimens, and therefore, overall buckling always occurred in compression. However, test data at least shows the general outline of the entire hysteretic response in the second and fourth quadrants.

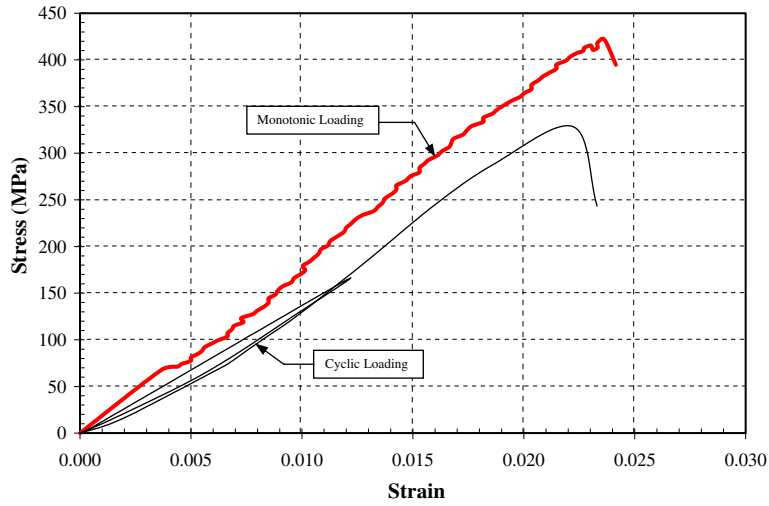


Fig. 6. Typical response of W series in compression.

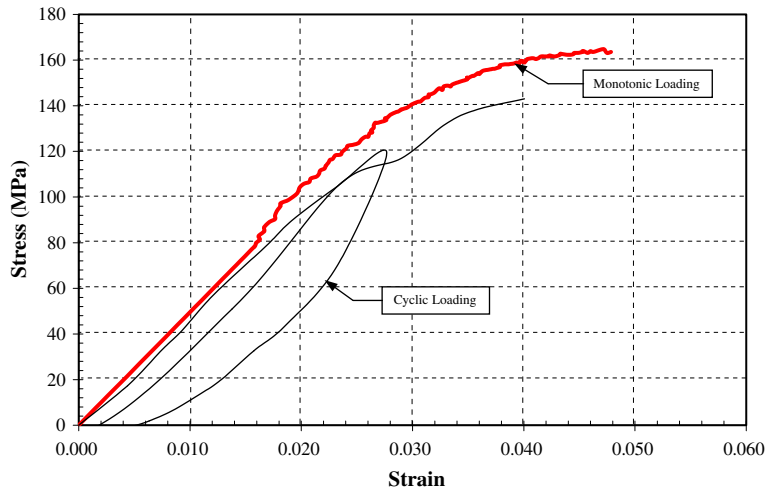


Fig. 7. Typical response of Y series in compression.

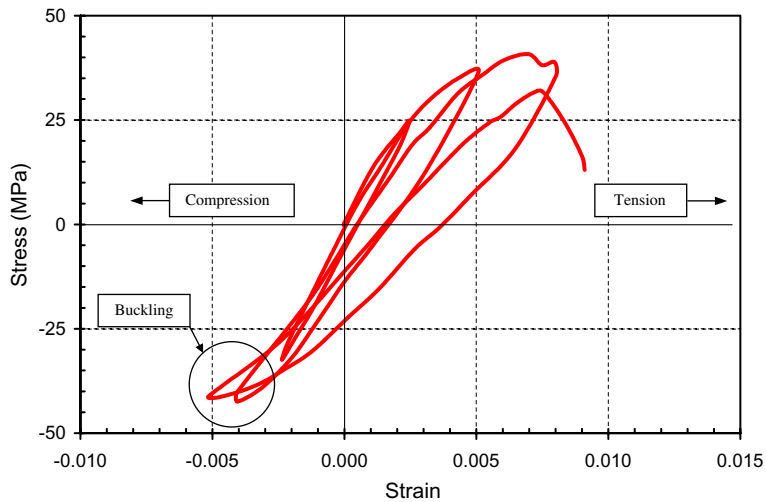


Fig. 8. Typical response of Y series in reverse cyclic loading.

This is very helpful in the full cyclic modeling of the Y series, as will be discussed in the next section.

4. Analytical modeling

4.1. Modeling of FRP laminate

As shown in Figs. 4 and 6, response of the W series was generally linear in both tension and compression. For modeling purposes, the energy dissipation and plastic strains of the W series were completely neglected, and it was assumed that the material was linear elastic, however, with different elastic moduli in tension and compression, as summarized in Table 3.

On the other hand, Figs. 5, 7, and 8 showed a parabolic response for the Y series in tension and compression. Fig. 9(a) and (b) show the test data (small circles) and the proposed models (solid lines) for the monotonic

response of the Y series in tension and compression, respectively. In both tension and compression, the monotonic response is assumed to be parabolic, as

$$f_j = 24,130 \cdot \varepsilon_j \cdot (1 - 114 \cdot \varepsilon_j) \quad (\text{stress in MPa}) \quad (1)$$

$$f_j = 6895 \cdot \varepsilon_j \cdot (1 - 10.5 \cdot \varepsilon_j) \quad (\text{stress in MPa}) \quad (2)$$

where f_j and ε_j are the stress and strain for the FRP, respectively. In modeling the response of the Y series for the full spectrum of cyclic loading, the following observations were made from Figs. 5, 7, and 8:

- Both the unloading and reloading branches can be described as parabolic curves, similar to the envelope curve, as

$$f_j = k_1^{u/r} \varepsilon_j^2 + k_2^{u/r} \varepsilon_j + k_3^{u/r} \quad (3)$$

where $k_i^{u/r}$ ($i = 1, 2, \text{ and } 3$) are the coefficients with superscripts u or r for unloading or reloading, respectively. Since FRP is used as reinforcement,

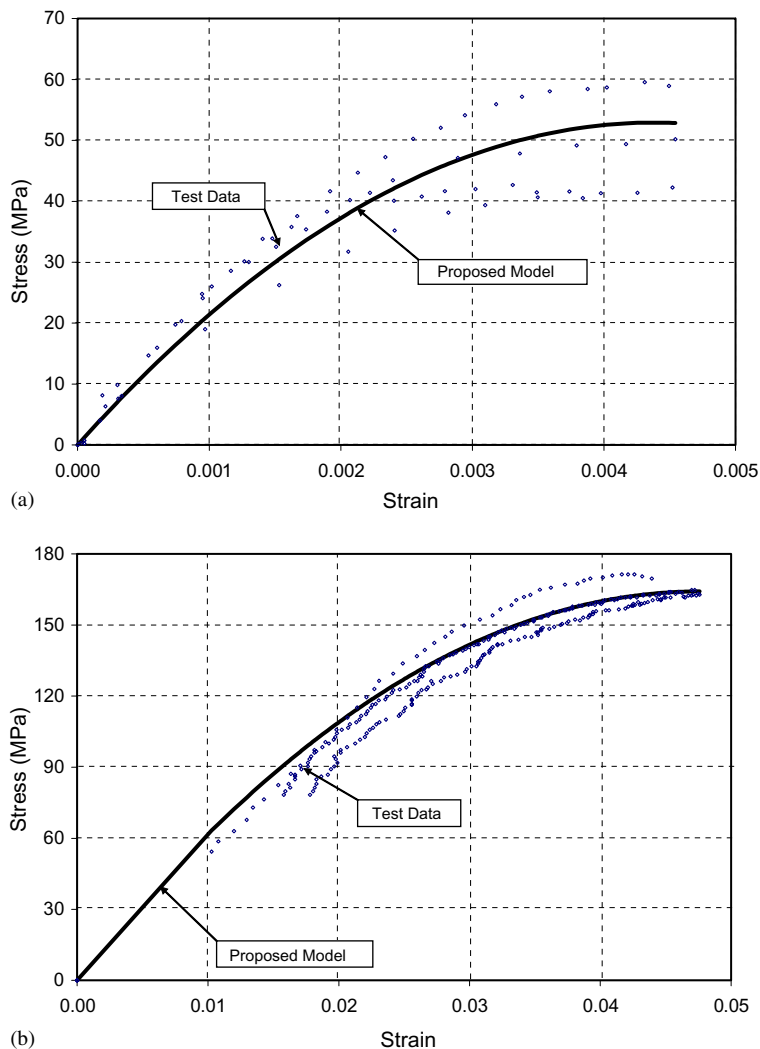


Fig. 9. Proposed model for Y series under monotonic loading: (a) tension and (b) compression.

unloading is considered from tension, whereas reloading is from compression.

- Little strength or stiffness degradation is apparent in the reloading branch.
- The unloading and reloading branches target the ultimate stress level in the opposite direction. The stress reversal tests showed the unloading branch in one direction to target the envelope curve in the other direction, rather than returning to the origin. This phenomenon was also confirmed from the behavior of the tubes of the Y series filled with concrete in the column tests. Return of the unloading branches to the origin would have resulted in an overwhelming pinching effect in the response of the concrete-filled FRP tubes of the Y series. No such pinching, however, was observed in the experiments even without internal steel reinforcement, as shown in Fig. 2.
- Tangent slopes of the unloading and reloading branches at the immediate start point is twice that of the secant slope between the start point and the ultimate stress level in the reversed direction.
- The reloading branch from an arbitrary stress level targets the last unloading point, and asymptotes back to the envelope curve with a common tangent.

Fig. 10 shows the full hysteretic response of the Y series, based on the above discussion. Coefficients in Eq. (3) can be found using the boundary conditions for the unloading and reloading branches, as described above:

$$k_1^u = -\frac{f_{uc} - f_{un}}{(\epsilon_{uc} - \epsilon_{un})^2} \quad (4)$$

$$k_2^u = -2 \cdot \frac{f_{uc} - f_{un}}{(\epsilon_{uc} - \epsilon_{un})^2} \cdot \epsilon_{uc} \quad (5)$$

$$k_3^u = f_{uc} - k_7 \cdot \epsilon_{uc}^2 - k_8 \cdot \epsilon_{uc} \quad (6)$$

$$k_1^r = -\frac{f_{ut} - f_{re}}{(\epsilon_{ut} - \epsilon_{re})^2} \quad (7)$$

$$k_2^r = -2 \cdot \frac{f_{ut} - f_{re}}{(\epsilon_{ut} - \epsilon_{re})^2} \cdot \epsilon_{ut} \quad (8)$$

$$k_3^r = f_{ut} - k_7 \cdot \epsilon_{ut}^2 - k_8 \cdot \epsilon_{ut} \quad (9)$$

where f_{ut} and f_{uc} are the ultimate tensile and compressive strengths of the tube, respectively, and ϵ_{ut} and ϵ_{uc} are the ultimate tensile and compressive strains of the tube, respectively.

4.2. Modeling of hybrid FRP-concrete columns

A fiber element model was adopted for the analysis of hybrid FRP-concrete columns [12], using a composite element that was initially developed for concrete-filled steel tubes [13]. The fiber element is a two-dimensional three-node combined element with 13 degrees of freedom, including five at each end node and three at the middle node. The generalized element consists of two frame elements for the concrete core and the FRP tube.

The model assumes perfect bond between concrete and FRP, and neglects creep of FRP and creep and shrinkage of concrete for the short-term cyclic loading. The model uses the Kirchhoff beam theory, higher order quartic Hermitian shape functions for transverse displacements, and quadratic Lagrangian shape functions for axial deformations. The tangent stiffness matrix for the combined element is derived using the virtual work approach, and by differentiating the internal nodal forces with respect to the nodal displacements. Details of the model are described in [12,13]. The fiber element model was incorporated into a general purpose nonlinear finite element analysis program (FEAP), which was

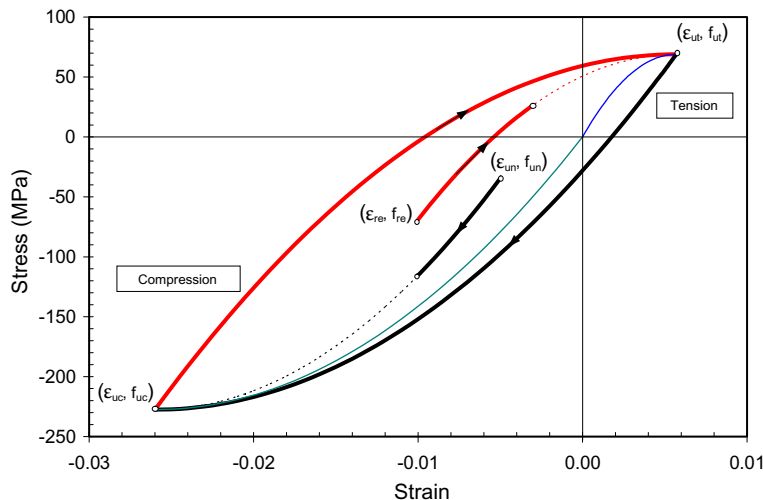


Fig. 10. Proposed cyclic model for Y series.

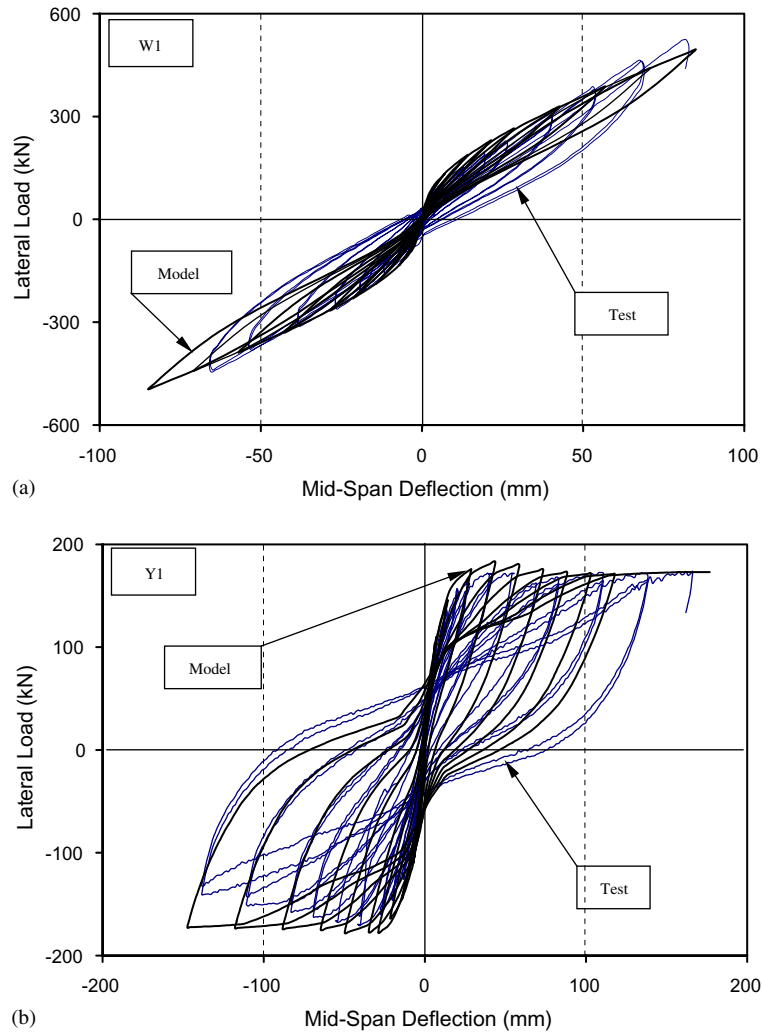


Fig. 11. Compression of the proposed model with test results for (a) specimen W1 and (b) specimen Y1.

initially developed by Professor Taylor at the University of California, Berkeley [14].

4.3. Model validation

Fig. 11 compares the fiber element analysis (solid lines) with test data (dashed lines) for specimens W1 and Y1, both without any internal steel reinforcement. The loading regime and the specimen configurations are shown in Fig. 1. The specimens were subjected to a constant axial load at about 6–10% of their axial capacity. Due to symmetry, only one half of each specimen was modeled, and only with two elements. It is observed that, in general, there is a good agreement between the analytical and experimental results. The agreement is closer for the Y series, as compared to the W series. The slight discrepancy for the W series is observed primarily in the reverse loading around the origin, indicating that the model predicts higher pinching than the actual tests for the W series. This may be

attributed to the use of the linear constitutive model for the FRP tube in the W series, which neglects the slight residual or plastic strains that were observed in the coupon tests for that series.

5. Conclusions

The implications of using FRP as primary and sole reinforcement for concrete structures in seismic regions was studied, in light of the fact that FRP materials are generally known for their linear elastic response to failure. An experimental and analytical investigation was carried out on the cyclic response of two different types of laminated glass FRP tubes filled with concrete. The two types of tubes represented two different failure modes; a brittle compression failure for the thick tubes with majority of the fibers in the longitudinal direction, and a ductile tension failure for the thin tubes with off-axis fibers. The experiments included coupons of the

tubes as well as large-scale specimens of the concrete-filled FRP tubes. The study showed that concrete-filled FRP tubes can be designed with an appropriate laminate structure for a ductility level comparable to that of conventional reinforced concrete columns. The nonlinearity and ductility in these types of structures stem from the off-axis response of the FRP tube. A hysteretic model was developed for the tube, and was cast into a two-dimensional three-node combined fiber element for the concrete-filled tube. Good agreement was shown between the analytical models and the experimental results.

Acknowledgements

This study was sponsored by the National Science Foundation (NSF) and the Florida Department of Transportation (FDOT). Additional support in the form of materials was provided by Owens Corning Corp and Smith Fiberglass Corp. The views and findings reported here are those of the authors alone, and not necessary those of the sponsoring agencies.

References

- [1] Mirmiran A, Shao Y, Shahawy M. Analysis and field tests on the performance of composite tubes under pile driving impact. *Compos Struct* 2002;55(2):127–35.
- [2] Brinson HF. A nonlinear visco-elastic approach to durability predictions for polymer based composite structures. In: Cardon AH, Verchery G, editors. *Proceedings of the Conference on Durability of Polymer Based Composite Systems for Structural Applications*, 1991. p. 46–64.
- [3] AASHTO. *Standard specifications for highway bridges*. 17th ed. Washington, DC: American Association of Highway and Transportation Officials; 2001.
- [4] Seible F, Burgueño R, Abdallah MG, Nuismer R. Development of advanced composite carbon shell systems for concrete columns in seismic zones. In: *Proceedings of the 11th World Conference on Earthquake Engineering*. Oxford, England: Pergamon, Elsevier Science Ltd.; 1996. Paper no. 1375.
- [5] Zhuo W, Fan L, Xue Y. Shaking table testing of simply supported bridges with prefabricated GFRP tube jacketed RC columns. In: Teng JG, editor. *Proceedings of the International Conference on FRP Composites in Civil Engineering*, Hong Kong, vol. II, 2001. p. 1337–44.
- [6] Yamakawa T, Komesu K, Zhong P, Satoh H. seismic performance of aramid fiber square tubed concrete columns with non-metallic reinforcement. In: Teng JG, editor. *Proceedings of the International Conference on FRP Composites in Civil Engineering*, Hong Kong, vol. II, 2001. p. 1329–36.
- [7] Hahn T, Tsai S. Nonlinear elastic behavior of unidirectional composite laminae. *J Compos Mater* 1973;7(1):102–18.
- [8] Hahn T. Nonlinear behavior of laminated composites. *J Compos Mater* 1973;7(4):257–71.
- [9] Hu H. Buckling analyses of fiber-composite laminate shells with material non-linearity. *J Compos Technol Res* 1993;15(3):202–8.
- [10] Haj-Ali R, Kilic H. Nonlinear behavior of pultruded FRP composites. *Compos Part B: Eng* 2002;33:173–91.
- [11] Yuan H, Xue Y, Li X, Zhang M. Study on a novel hybrid GFRP/CFRP composite beam. In: *Proceedings of the 2nd Chinese National Conference of Application Technology of FRP Materials in Civil Engineering*, Kunming, China. Beijing, China: Tsinghua University Publication; 2002. p. 296–305 [in Chinese].
- [12] Shao Y. Behavior of FRP-concrete beam-columns under cyclic loading. PhD thesis, North Carolina State University, Raleigh, NC, 2003 [also, see under the same title: Shao Y, Mirmiran A. NCSU-CFL Report No. RD-03-02, 2003].
- [13] Aval SBB, Saadeghvaziri MA, Golafshani AA. Composite inelastic fiber element for cyclic analysis of concrete-filled steel tube columns. *J Eng Mech, ASCE* 2002;128(4):428–37.
- [14] Taylor RL. FEAP—A finite element analysis program. Manual, Department of Civil Engineering, University of California, Berkeley, CA, 1998.